Mechanism of the Bis(imino)pyridine Iron-Catalyzed Hydromagnesiation of Styrene Derivatives

Peter G. N. Neate,[†,§] Mark D. Greenhalgh,[§] William W. Brennessel,[†] Stephen P. Thomas*[,§] and Michael L. Neidig*[,†]

[§]EaStCHEM School of Chemistry, University of Edinburgh, David Brewster Road, Edinburgh, UK, EH9 3FJ
[†]Department of Chemistry, University of Rochester, Rochester, New York 14627, United States

ABSTRACT: Iron-catalyzed hydromagnesiation of styrene derivatives offers a rapid and efficient method to generate benzylic Grignard reagents, which can be applied in a range of transformations to provide products of formal hydrofunctionalization. Whilst iron-catalyzed methodologies exist for the hydromagnesiation of terminal alkenes, internal alkynes and styrene derivatives, the underlying mechanisms of catalysis remain largely undefined. To address this issue, and determine the divergent reactivity from established cross-coupling and hydrofunctionalization reactions, a detailed study of the bis(imino)pyridine iron-catalyzed hydromagnesiation of styrene derivatives is reported. Using a combination of kinetic analysis, deuterium labelling and reactivity studies, as well as *in situ* ^{57}Fe Mössbauer spectroscopy, key mechanistic features and species were established. A formally iron(0) ate complex [^{iPr}BIPFe(Et)(CH_2=CH_2)]$^-$ was identified as the principle resting state of the catalyst. Dissociation of ethene forms the catalytically active species which can reversibly coordinate the styrene derivative and mediate a direct and reversible β-hydride transfer, negating the necessity of a discrete iron-hydride intermediate. Finally, displacement of the tridentate bis(imino)pyridine ligand over the course of the reaction results in the formation of a tris-styrene-coordinated iron(0) complex, which is also a competent catalyst for hydromagnesiation.

1. INTRODUCTION

Hydrofunctionalization of unsaturated carbon-carbon bonds represents a powerful method for building molecular complexity from inexpensive and widely accessible chemical feedstocks. Recently, the iron-catalyzed hydromagnesiation of alkenes and alkynes has emerged as an effective and widely applicable method for their formal hydrofunctionalization in high yield and with control of regio- and stereochemistry.[1–4] The resulting Grignard reagents are highly reactive and versatile nucleophiles which can be exploited in synthesis, by way of their direct reaction with a range of electrophiles as well as their application in subsequent catalytic reactions such as Kumada-Tamao-Corriu cross-coupling.[5]

Iron-catalyzed alkene hydromagnesiation was first reported by Copper and Finkbeiner in 1962,[6] later being observed by Kochi and coworkers during their pioneering work on cross-coupling.[7,8] However, whilst illustrating the principle, the yields in these early reports were poor and therefore did not represent viable synthetic procedures. It was not until 2012 that the potential of iron-catalyzed hydromagnesiation was truly exploited, with three complementary procedures reported (Scheme 1).[9–11] Shirakawa and Hayashi reported an iron and copper co-catalyzed system for the linear selective hydromagnesiation of terminal alkyl-substituted alkenes;[9] Thomas reported the branched-selective hydromagnesiation of styrene derivatives;[11–13] and Nakumura reported the hydromagnesiation of diaryl alkynes. Despite these synthetic advances, the mechanistic underpinnings of iron-catalyzed hydromagnesiation remains largely unknown. An in-depth mechanistic understanding of these reactions would not only allow further development of these methods, but also provide valuable insight into other iron-catalyzed reactions that are carried out under similar, highly reducing conditions such as cross-coupling, carbometallation and dehalogenation.[14–21] Importantly, the insight gathered would also extend to general hydrofunctionalization chemistry, an area in which bis(imino)pyridine iron complexes have been extensively applied, including under activation using EtMgBr.[2,22]

Scheme 1. Iron-catalyzed hydromagnesiation of alkyl-alkenes, aryl-alkenes and alkynes.

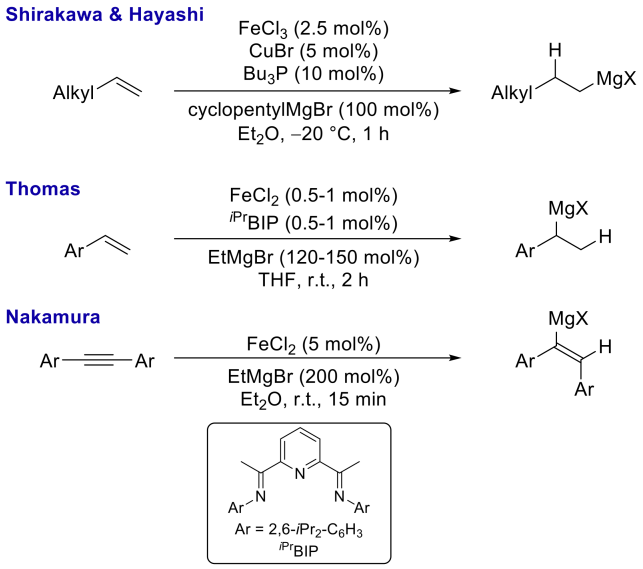

At present, mechanistic insight has been limited to that gained as part of methodology development. Net hydride transfer is the key step in the hydromagnesiation reaction and has

been proposed to proceed by alkene hydrometallation by an iron-hydride. Kochi originally proposed a discreet iron-hydride as the catalysts for hydromagnesiation.[8] Shirakawa and Hayashi also proposed the intermediacy of an iron-hydride in the iron and copper co-catalyzed isomerization of Grignard reagents,[23] and by extension hydromagnesiation. Likewise, Thomas favored a hydrometallation pathway.[11] The intermediacy of an iron-hydride has also been proposed for the isomerization of 3-coordinate iron(II)-alkyl complexes.[24,25] In contrast, a recent DFT study proposed the reaction proceded by a direct β-hydride transfer between ethyl and styrene ligands on iron, without the intermediacy of an iron-hydride.[26] This type of hydride transfer has also been proposed for nickel-catalyzed hydromagnesiation.[27–29] However, it should be noted that these computions were based on an iron(II) cycle, which is unlikely under the highly reducing conditions of the reaction.

Thus, we sought to gain molecular-level insight into the mechanism of bis(imino)pyridine-iron-catalyzed hydromagnesiation of styrene derivatives. In the current study, key questions were addressed through the combined use of kinetic analysis, deuterium labelling studies and *in situ* ^{57}Fe Mössbauer spectroscopy. These questions included the mechanism of hydride transfer, whether direct or proceeding through an intermediate iron-hydride; iron speciation in stoichiometric and catalytic reactions as well as the identity of these key intermediates and their implication during catalysis.

2. RESULTS AND ANALYSIS

2.1. Hydride Transfer: Reversibility, Selectivity and Mechanism

We began by investigating the homogeneity of the hydromagnesiation reaction using bis(imino)pyridine ligated iron pre-catalysts by selective inhibition studies[30–36] and a three-phase test[37,38](see Supporting Information, Section 3). Hydromagnesiation of a polymer-bound styrene substrate was successful; whilst the addition of dibenzo[*a*,*e*]cyclooctatetraene (DCT) to a model reaction resulted in almost instanteous inhibition. Both of these studies are consistent with the operation of a homogeneous iron catalyst.

The hydromagnesiation of 2-methoxystyrene catalyzed by $FeCl_2$/^{iPr}BIP with a variety of Grignard reagents was used to examine the initial rates of reactions and regioselectivity of hydride transfer over the course of the reaction (Scheme 2). Notably, the intial rate of reaction and product regioselectivity was highly dependent on the structure of the Grignard reagent used (see Supporting Information, Section 4). Whilst EtMgBr efficiently catalyzed the reaction, the use of *i*-BuMgBr provided an initital rate of reaction three orders of magnitude lower. This is in stark contrast to titanium-catalyzed hydromagnesiation, where *i*-BuMgBr was reported to be most efficient at forming the key Ti-H intermediate.[39] For all the Grignard reagents tested, the branched to linear regioselectivity (α-aryl- to β-aryl, respectively, as determined by trapping with DMF) of the product increased over the course of the reaction, suggesting that any β-aryl Grignard reagent formed was isomerized to the thermodynamically favored α-aryl Grignard reagent.

To investigate this possibility, a β-aryl Grignard reagent was used. This resulted in efficient hydromagnesiation of 2-methoxystyrene, albeit with decreased regioselectivity, showing the competence of the linear Grignard reagent as a hydride donor (Scheme 2). In all cases an initial preference for the α-aryl Grignard reagent was observed, suggesting the α-aryl Grignard reagent is kinetically and thermodynamically favored. The observation that the Grignard reagent structure has a significant influence on regioselectivity is not easily reconcilable with the proposal of a common iron-hydride intermediate being operative.[9,11,23]

Scheme 2. Hydromagnesiation of 2-methoxystyrene using different Grignard reagents.

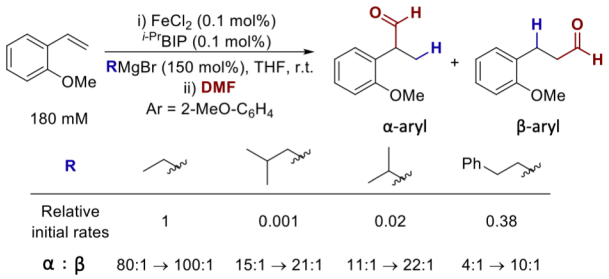

The hydromagnesiation of 2-methoxystyrene using d_5-EtMgBr and d_7-^{i}PrMgBr was used to confirm the influence of the Grignard reagent on the selectivity of hydride transfer and reversibility of this process (Scheme 3, see Supporting Information, Section 5).

Scheme 3. Hydromagnesiation of 2-methoxystyrene using deuterated Grignard reagents.

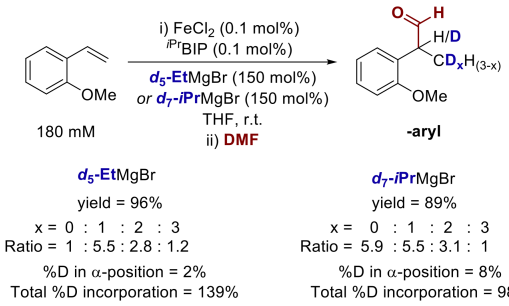

Using d_5-EtMgBr, the incorporation of 0 or 1 deuterium at the terminal carbon of the trapped hydromagnesiation product, α-aryl aldehyde, was observed from the outset of the reaction, with 2 or 3 deuterium observed only as the reaction progressed. Very little deuterium incorporation was observed at the α-position (< 2%). In contrast when d_7-^{i}PrMgBr was used the major products were those with only 0 or 1 deuterium in the β-position, whilst significantly higher deuterium incorportation was observed at the α-position. These observation are consistent with the regioselectivity of hydromagnesiation observed using different Grignard reagents, and the ability of the β-aryl Grignard reagent to undergo isomerization to the α-aryl Grignard reagent. For both Grignard reagents, the concentration of each deuterium-incorporated α-aryl Grignard reagent increased to a constant concentration, suggesting that the α-aryl Grignard reagent did not re-enter the catalytic cycle. Additionally using either deuterated Grignard reagent, deuterated styrene derivatives were observed during the early stages of reaction, with their subsequent consumption over time. These observations demonstate that both hydride transfer and styrene coordination are reversible.

Additionally, using d_5-EtMgBr, a kinetic isotope effect of 1.3 was observed for the hydromagnesiation of 4-*tert*-butylstyrene and 3-methoxystyrene (see Supporting Information, Section 6). The observation of a kinetic isotope effect indicates that hydride transfer occurs prior to the rate-limiting step but its magnitude, along with the observed reversibility of hydride transfer, excludes hydride transfer as the rate-limiting step. Kinetic isotope effects of this magnitude have previously been reported with reversibility of the process accounting for the observed value.[40]

Scheme 4. Possible mechanisms for the iron-catalyzed isomerization of (2-phenylethyl)magnesium bromide.

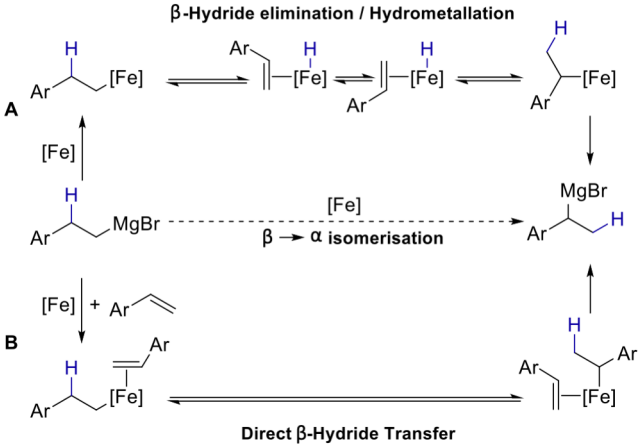

Two mechanisms of hydride transfer have been proposed for hydromagnesiation using other metals. The titanium-catalyzed hydromagnesiation of alkenes, dienes and alkynes was proposed to proceed through a titanium-hydride intermediate, generated by β-hydride elimination of a titanium-alkyl precursor.[6,39,41–49] In contrast, nickel-catalyzed alkene hydromagnesiation has been proposed to proceed by direct β-hydride transfer from a nickel-alkyl species.[28] Thus we wished to gain definitive insight into the mechanism of hydride transfer in iron-catalyzed hydromagnesiation. As the observation that the Grignard reagent had a significant influence on the regioselectivity contrasts proposals of a common iron-hydride intermediate (*vide supra*), the isomerization of a β-aryl Grignard reagent was investigated (Scheme 4). In principle, if an iron-hydride intermediate was the active hydromagnesiation species, the β-aryl Grignard reagent would isomerize to the corresponding α-aryl Grignard reagent in the presence of the iron catalyst alone (Scheme 4, A). In contrast, if hydromagnesiation proceeded by a direct hydride transfer mechanism, then isomerization would only take place in the presence of a styrene (or alkene) derivative capable of undergoing hydromagnesiation (Scheme 4, B).

The reaction of $Ph(CH_2)_2MgBr$ with ^{iPr}BIPFeCl$_2$ (0.1 mol%) gave only 1% isomerization to the α-aryl Grignard reagent over 5 hours (Figure 1, ●).[50] Significantly, the addition of styrene (10 mol%, Figure 1, ●) promoted the isomerization to provide 23% of α-aryl Grignard reagent in the same time period. Alternatively, the isomerization could also be promoted by 1-octene (100 mol%, Figure 1, ●). To ensure an alkene was not simply required for catalyst stabilization, alkenes (including styrene derivatives) unable to undergo hydromagnesiation were added to the reaction with no isomerization observed.[51] The observation that isomerization only occurred in the presence of an alkene capable of undergoing hydromagnesiation supports the operation of a direct β-hydride transfer mechanism (Scheme 4. B). A similar mechanism has been suggested by Ziegler and coworkers as the main chain transfer process in bis(imino)pyridine iron-complex catalyzed polymerization.[52]

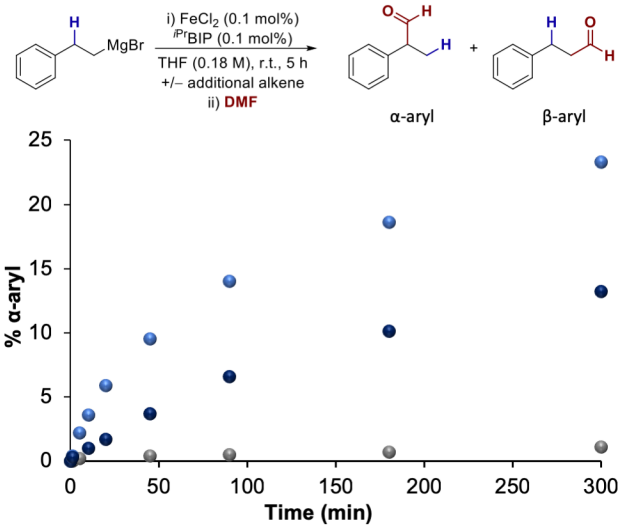

Figure 1. Isomerization of (2-phenylethyl)magnesium bromide. ● = no alkene added (0.5 mol% styrene present in Grignard reagent); ● = Styrene (10 mol%) added; ● = 1-Octene (100 mol%) added.

2.2 *In situ* Iron Speciation in Reactions with Grignard Reagent

The reaction of ^{iPr}BIP^{57}FeCl$_2$ with EtMgBr was carried out in THF at −17 °C, with samples freeze-quenched in liquid nitrogen after two minutes. On reaction with 2 and 3 equivalents of EtMgBr, Mössbauer spectra showed complex mixtures of ≥ 3 species (see Supporting Information Section 8.1). However,

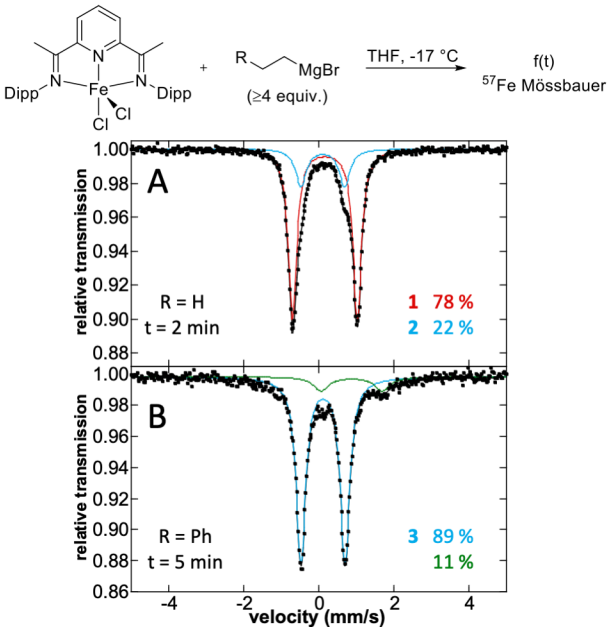

Figure 2. 80 K frozen solution Mössbauer spectrum of the reaction of ^{iPr}BIP^{57}FeCl$_2$ with A) 4 equiv. EtMgBr at for 2 minutes; B) 10 equiv. $Ph(CH_2)_2MgBr$ for 5 minutes.

adding 4, 5 or even 20 equivalents of EtMgBr resulted in almost identical Mössbauer spectra, which showed only two species (Figure 2, A).

The major species **1**, in all cases, constitutes ~80% of all iron in solution and has Mössbauer parameters of $\delta = 0.16$ mm/s and $\Delta E_Q = 1.72$ mm/s (Figure 2, A, red). The second species **2**, which constitutes the remaining ~20% of iron in solution, displayed Mössbauer parameters of $\delta = 0.11$ mm/s and $\Delta E_Q = 1.18$ mm/s (Figure 2, A, blue).[53] Carrying out the analogous reaction using $^{57}FeCl_2$ and ^{iPr}BIP, rather than the preformed complex, resulted in the same two species being observed and in similar quantities. Both species have Mössbauer parameters in the region of previously reported reduced formally iron(0) to iron(−II) bis(imino)pyridine iron complexes.[54–56]

Reaction of ^{iPr}BIPFeCl$_2$ with 4 equivalents EtMgBr at −17 °C followed by addition of hexane and standing at −30 °C gave the iron-ethyl-ethene complex [^{iPr}BIPFe(Et)(H$_2$C=CH$_2$)][MgX(THF)$_5$], as characterized by single crystal X-ray diffraction (Figure 3, A). Mössbauer parameters of the isolated crystalline material were consistent with complex **1**, the major species generated *in situ* from the reaction of ^{iPr}BIPFeCl$_2$ with ≥ 4 equivalents of EtMgBr (Table 1). The slight changes in parameters suggest a slight structural distortion between solid and solution states. A similar reaction of ^{iPr}BIPFeCl$_2$ with excess Ph(CH$_2$)$_2$MgBr (10 equiv.) gave single crystals suitable for X-ray diffraction, identified as the iron-alkyl-dinitrogen complex [^{iPr}BIPFe(N$_2$)(CH$_2$CH$_2$Ph)][MgX(THF)$_5$] **3** (Figure 3, B). Mössbauer spectroscopy of isolated, crystalline **3** exhibited the same parameters to that of the major species observed in situ on reaction with Ph(CH$_2$)$_2$MgBr (Table 1; Figure 2, B, blue). The remaining 11% of iron in solution for the *in situ* reaction corresponding to a species with Mössbauer parameters $\delta = 0.88$ mm/s and $\Delta E_Q = 1.63$ mm/s (Figure 2, B, green).

The electronic structure of iron complexes of this ligand class, including their reduced forms, have been extensively studied by Chirik and coworkers.[54–58] Based on these studies, complexes **1** and **3** are designated as formal iron(0) complexes, where the redox activity of the ligand may result in some contribution from resonance hybrid structures. Consistent with this assignment, both complexes display the characteristic elongation of C_{imine}-N_{imine} bonds (1.274(3) Å to 1.3647(18) and 1.3624(19) Å for complex **1**; and 1.381(9) and 1.384(10) Å for complex **3**),[54] and contraction of the C_{imine}-C_{ipso} bonds (1.489(3) and 1.487(3) Å to 1.409(2) and 1.408(2) Å for complex **1** and 1.385(14) and 1,428(12) complex **3**). The degree of asymmetry in complex **3** is more pronounced than in previously isolated formally iron(0) complexes, the origin of which would require a detailed electronic structure study to understand. Additionally of note is the elongation of the ethene bond in complex **1** (from 1.330 to 1.406(2) Å) illustrating the high degree of π-backbonding present.[59] The dinitrogen bond length in complex **3** is consistent with minimal activation by the iron center as previously reported by Chirik *et al.*, which they additionally corroborated using infrared spectroscopy.[57]

The fact that complex **3** exhibits the same Mössbauer parameters as complex **2**, the minor species generated on reaction of ^{iPr}BIPFeCl$_2$ with EtMgBr, suggests that complex **2** is analogous to complex **3**, with an ethyl moiety bound as well as a molecule of dinitrogen. The fact that a species analogous to complex **1** was not observed upon reaction of ^{iPr}BIP^{57}FeCl$_2$ with Ph(CH$_2$)$_2$MgBr suggests that styrene coordination to an iron-alkyl complex is thermodynamically unfavorable, potentially due to the increased steric hindrance introduced by styrene, relative to ethene.

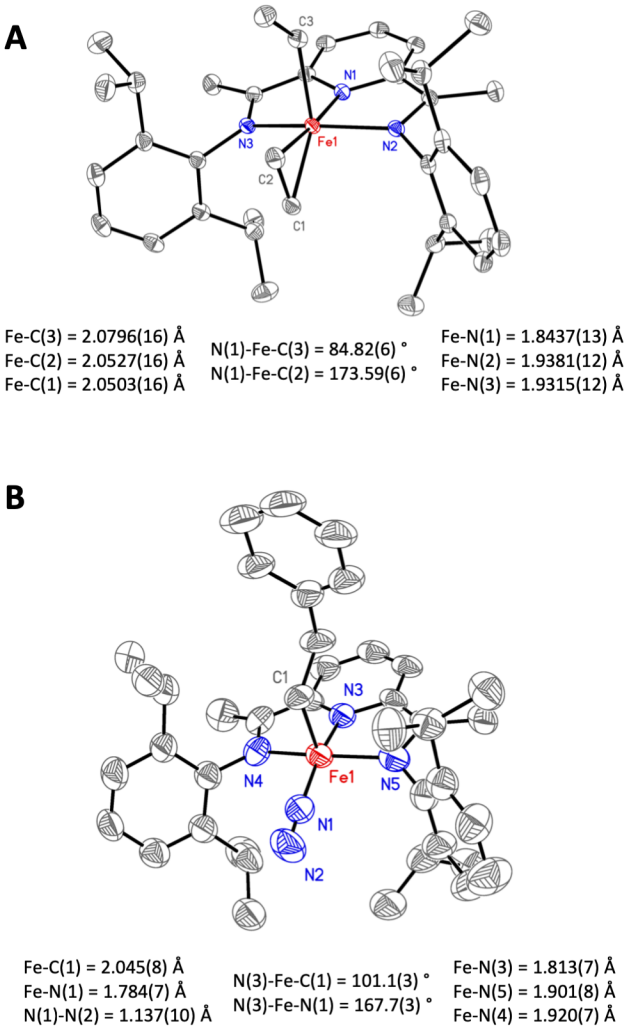

Figure 3. X-Ray crystal structures of A) [^{iPr}BIPFe(Et)(CH$_2$=CH$_2$)][MgX(THF)$_5$] **1** and B) [^{iPr}BIPFe(N$_2$)(CH$_2$CH$_2$Ph)][MgX(THF)$_5$] **3**. Structures drawn with thermal displacement ellipsoids at 50 % probability level. Iron shown in red; nitrogen atoms in blue; carbon in grey and hydrogen atoms omitted for clarity. Note: magnesium countercation omitted for clarity.

Ethene being bound to the iron center in complex **1** indicates that reduction of ^{iPr}BIPFeCl$_2$ occurs through a β-hydride elimination process. This can be envisioned to take place by initial rapid transmetallation of ^{iPr}BIPFeCl$_2$ with two equivalents of the relevant Grignard reagent, which is added in excess and rapidly, to produce the iron bis-alkyl species. β-hydride elimination would give an iron-hydride species and an equivalent of the appropriate alkene. Subsequent reductive elimination of the hydride and alkyl moiety would provide the required two-electron reduction as well as the alkane byproduct. An analogous reduction pathway was proposed by Tamura and Kochi, where the alkene and alkane byproducts of the reaction were tracked.[7,8] This type of reduction has also been proposed for the reaction

of bis(diisopropylphosphino)propane iron(II) chloride with excess EtMgBr.[60,61] In contrast to the iron-ethyl-ethene complex formed here, the bisphosphine iron(0) complex gave a bis ethylene complex, albeit in excess ethylene. The contrasting speciation points towards the $^{i\text{Pr}}$BIP ligand influencing the relative affinity of the iron center towards binding either an alkyl or alkene moiety.

It is noteworthy that during the development of the catalytic protocol, it was demonstrated that reactivity was not observed at temperatures ≤ 0 °C.[11] Reaction of $^{i\text{Pr}}$BIP^{57}FeCl$_2$ with EtMgBr (20 equiv.) at 10 °C and 20 °C revealed the same two iron species as those observed at −17 °C, with complex **1** constituting 68% and 60% of iron in solution at 10 and 20 °C, respectively, and complex **2** accounting for the remaining iron in solution in both cases.

At slightly longer time-points (80 seconds at 20 °C), both **1** and **2** are present in roughly equal ratios, although broadening of the Mössbauer spectrum is observed. This broadening is indicative of decomposition of **1** and **2** at elevated temperatures and excess EtMgBr.

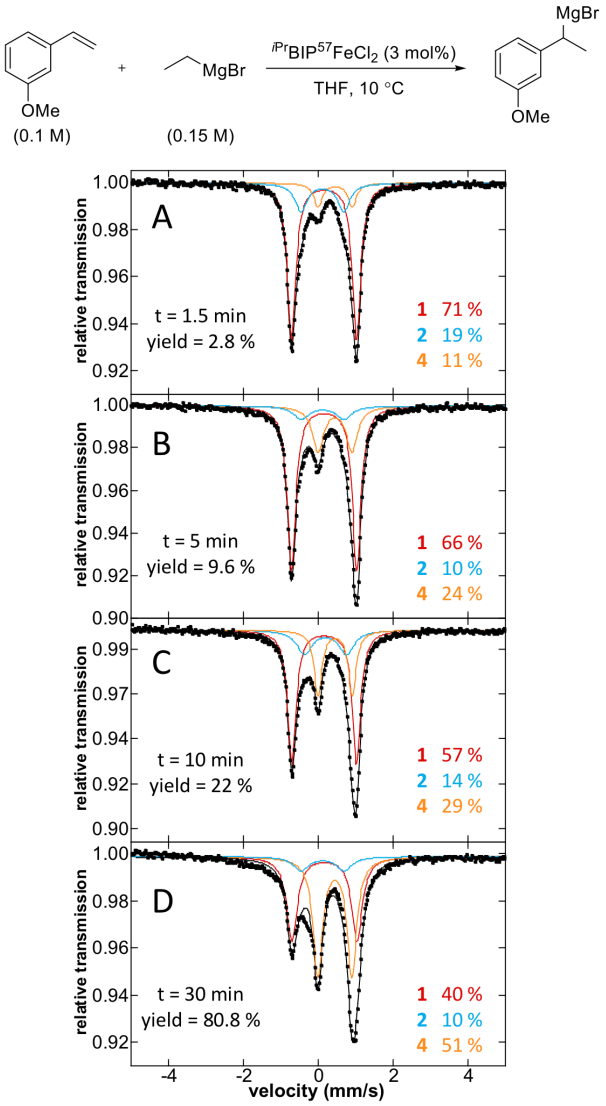

Figure 4. 80 K frozen solution Mössbauer spectra taken during hydromagnesiation of 3-methoxystyrene.

2.3 *In situ* Iron Speciation During Catalysis

Beyond stoichiometric reactions of $^{i\text{Pr}}$BIP^{57}FeCl$_2$ with Grignard reagents, it was also important to evaluate iron speciation during catalysis. Preliminary investigations towards interrogating reaction kinetics found that the shape of the reaction profile was significantly affected by the choice of styrene derivative (see Supporting Information, Section 10). On this basis, *in situ* freeze-quenched Mössbauer spectroscopy was undertaken using two representative styrene derivatives: 3-methoxystyrene and 4-*tert*-butylstyrene. Representative samples using each styrene derivative were prepared for Mössbauer spectroscopy by freeze-quenching analogous reactions at specific time points to provide a picture of how the iron speciation varies over time (see Supporting Information, Section 8.3).

In the reactions with 3-methoxystyrene, three species were observed over the course of the reaction (Figure 4). Initially the major species, constituting 71% of iron in solution, is the iron-ethyl-ethene complex **1**. The concentration of complex **1** gradually decreases to 40% over the course of 30 minutes (Figure 4A→D, red). Also present during catalysis is the iron-ethyl-dinitrogen complex **2**, the concentration of which remains relatively consistent throughout the reaction (10–14%) after decreasing slightly over the first few minutes (Figure 4A→D, blue).

A previously unobserved species, **4**, with Mössbauer parameters significantly different to those already identified (Table 1; δ = 0.44 mm/s and ΔE_Q = 0.88 mm/s) was observed to increase significantly over the course of the reaction (Figure 4, A→D, orange). Towards the end of the reaction (Figure 4, D) slight broadening of the Mossbauer spectrum is observed, consistent with decomposition to multiple, low concentration species.

Table 1. Summary of 80 K ^{57}Fe Mössbauer parameters of identified iron complexes.

Complex	Solid		Frozen Solution	
	δ (mm/s)	ΔE_Q (mm/s)	δ (mm/s)	ΔE_Q (mm/s)
1	0.16	1.66	0.16	1.72
2	-	-	0.11	1.18
3	0.11	1.19	0.11	1.18
4	0.44	0.89	0.44	0.88

Despite the difference in kinetic behavior for the hydromagnesiation of 4-*tert*-butylstyrene, the same three iron species were observed over the course of the reaction. However, their relative changes in concentration were much less pronounced (see Supporting Information, Section 8.3). Complex **1** was identified as the major species, representing ~70% of iron in solution at all time points. Complex **2** constituted ~20% at early time-points, with its concentration gradually decreasing over the course of the reaction. The unidentified species **4** was observed to gradually increase during catalysis. Whilst initially constituting ~5 % of iron in solution, ~20% of species **4** was present at later time-points (7-10 min; ~36% yield). Broadening of the Mössbauer spectrum at later time points (30 minutes, ~68% yield) was observed to a much greater extent than that observed with 3-methoxystyrene.

Having established the speciation of iron for the hydromagnesiation of different styrene derivatives, we next examined the effect of using a different Grignard reagent. $Ph(CH_2)_2MgBr$ was chosen as it was the second most kinetically competent Grignard reagent (Scheme 2), and the species generated by reaction with ^{iPr}BIPFeCl$_2$, iron-alkyl-dinitrogen complex **3**, had already been established. Freeze-quenched samples taken during the hydromagnesiation reaction showed the major species to be the iron-alkyl-dinitrogen complex **3**. Whilst initially constituting 85% of iron in solution, complex **3** decreased to 63% after 20 minutes (Figure 5, blue). The remaining iron in solution at both time-points was made up by the unidentified species **4**, previously observed during the hydromagnesiation reactions using EtMgBr (Figure 5, orange). The lack of a species analogous to iron-ethyl-ethene complex **1** being observed is consistent with the stoichiometric reaction studies and indicates the unfavorable nature of coordinating both a phenethyl group and a styrene derivative to the iron complex simultaneously (see Section 2.2).

As only these two species were observed during the hydromagnesiation reaction using $Ph(CH_2)_2MgBr$, crystallization attempts were undertaken to isolate complex **4**. Reaction of ^{iPr}BIPFeCl$_2$ with $Ph(CH_2)_2MgBr$ (10 equiv.) and an excess of styrene (20 equiv.) for 2 minutes at room temperature, followed by rapid cooling and storing at −80 °C gave crystalline material which was identified as a tris-styrene ligated iron(0)alkyl complex [Fe(η^2-styrene)$_3$(κ^1-CH(CH$_3$)Ph)][MgX(THF)$_5$], by single crystal X-ray diffraction (Figure 6). Unexpectedly, the ^{iPr}BIP ligand had been displaced in favor of three molecules of styrene, bound to an α-aryl-iron species, presumably formed as a result of styrene hydrometallation. ^{57}Fe Mössbauer spectroscopy of the crystalline complex exhibited parameters corresponding to the previously unidentified complex **4**, which was observed to increase in concentration during the catalytic hydromagnesiation reactions using either EtMgBr or $Ph(CH_2)_2MgBr$ (Table 1).

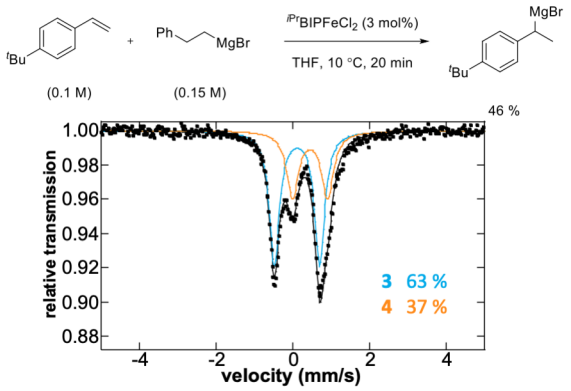

Figure 5. 80 K frozen solution Mössbauer spectrum taken 20 minutes into the hydromagnesiation reaction of 4-*tert*-butylstyrene using $Ph(CH_2)_2MgBr$.

The observation of complex **4** in greater quantities during hydromagnesiation reactions using 3-methoxystyrene is attributed to the greater binding affinity of more electron deficient styrene derivatives, which better stabilize the iron(0) center and prevent catalyst deactivation by aggregation.[62] By comparison, styrene derivatives bearing electron-donating groups, such as 4-*tert*-butylstyrene, would not be expected to stabilize an iron(0) species as effectively. As a result, aggregation occurs more readily, corresponding to the more pronounced broadening of Mössbauer spectra and the rapid decrease in catalytic activity (see Supporting Information, Section 8.3). The stronger binding of more electron-deficient styrene derivatives was supported by a competition experiment between 3-methoxystyrene and 4-*tert*-butylstyrene. While the hydromagnesiation of 3-methoxystyrene itself is slower than 4-*tert*-butylstyrene, when the hydromagnesiation reaction was carried out with a 1:1 mixture of the two, 3-methoxystyrene reacted preferentially (see Supporting Information, Section 11).

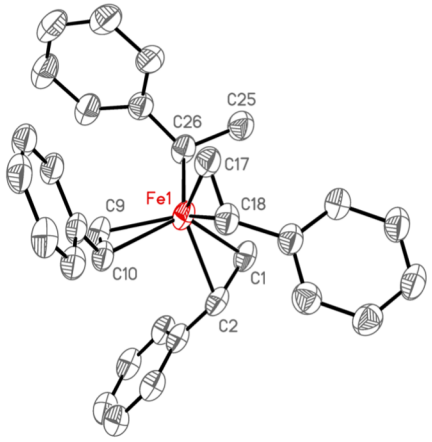

Fe-C(1) = 2.065(2) Å	C(26)-Fe-C(1) = 90.29(16) °	Fe-C(26) = 2.150(4) Å
Fe-C(2) = 2.209(2) Å	C(26)-Fe-C(2) = 123.23(16) °	C(25)-C(26) = 1.521(6) Å
Fe-C(17) = 2.056(3) Å	C(26)-Fe-C(17) = 95.22(18) °	C(1)-C(2) = 1.403(4) Å
Fe-C(18) = 2.233(3) Å	C(26)-Fe-C(18) = 129.27(17) °	C(17)-C(18) = 1.398(4) Å

Figure 6. X-Ray crystal structure of [Fe(η^2-styrene)$_3$(κ^1-CH(CH$_3$)Ph)][MgX(THF)$_5$] **4** and representative bond distances and angles. Structure drawn with thermal displacement ellipsoids at 50% probability level. Iron shown in red, carbon in grey and hydrogen atoms omitted for clarity. Note: magnesium counter-cation omitted for clarity.

2.4 Reactivity of Complexes 1 and 4

As the two significant species observed during the optimized catalytic reaction, it was important to evaluate the reactivity of complexes **1** and **4**. Use of complex **1** as a pre-catalyst (3.3 mol%) for the hydromagnesiation of 4-*tert*-butylstyrene with EtMgBr under standard catalytic conditions gave near quantitative yield after just 20 minutes at room temperature (Figure 7). The iron(0)-tris-styrene complex **4** exhibited comparable reactivity over the first three minutes of the reaction, after which its rate dropped off compared with reactions using ^{iPr}BIP. However, complex **4** was demonstrated to be a minor component in the reactions using ^{iPr}BIP, 13% of the iron in solution by freeze-quenched ^{57}Fe Mössbauer spectroscopy (see Supporting Information Section 9.4). This establishes that, in the presence of ^{iPr}BIP, the major reaction pathway proceeds through complex **1**.

Despite complex **4** being a minor component, we were curious whether effective catalysis could be achieved in the absence of ^{iPr}BIP. Carrying out the analogous reaction with $FeCl_2$ alone proved ineffective, affording ~15% yield even after one hour (Figure 7). Consistent with this the reaction of $^{57}FeCl_2$ with $Ph(CH_2)_2MgBr$ in the presence of styrene, even at –17 °C, resulted in a complex mixture of species by ^{57}Fe Mössbauer spectroscopy which may contain some small quantity of complex **4**.

This suggests that $^{i\text{Pr}}$BIP is not only necessary for achieving effective catalysis through generation of complex **1**, but also plays a role in the formation of complex **4**.

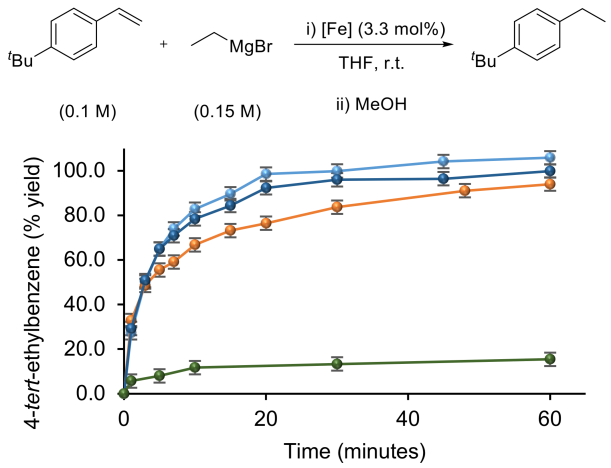

Figure 7. Hydromagnesiation of 4-*tert*-butylstyrene using isolated iron sources. ● = complex **1**; ● = $^{i\text{Pr}}$BIPFeCl$_2$; ● = complex **4**; ● = FeCl$_2$

As the major reactive species present during catalysis in the presence of $^{i\text{Pr}}$BIP, the reactivity of complex **1** was further examined. Stoichiometric reaction of complex **1** with 4-*tert*-butylstyrene or 3-methoxystyrene (6 equiv.), gave only trace product. However, carrying out the analogous reaction (5 equiv. 4-*tert*-butylstyrene) in the presence of EtMgBr (1 equiv.) gave 114 % product formation, with respect to iron. It should be noted that complex **1** did not react further with EtMgBr alone (Section 2.5). This precludes a different species, such as coordination of additional EtMgBr, being responsible for the observed reactivity. That turnover is only achieved in the presence of additional EtMgBr, in combination with this observation, suggests that additional EtMgBr is required for release of the product Grignard reagent.

Isolation of the iron-alkyl-dinitrogen complex **3**, devoid of a coordinated styrene, suggests that the coordination of both an alkyl moiety and styrene-derivative is disfavored due to steric constraints. To probe whether a styrene-coordinated intermediate can be observed and whether such a species precedes turnover, complex **1** was generated *in situ* in the presence of styrene (10 equiv.). No new iron species were observed. Upon warming, the concentration of iron-ethyl-dinitrogen complex **2** increased significantly to 45% of iron in solution after 5 minutes (see Supporting Information, Section 9.4). Approximately 2-3% of the iron(0)-tris-styrene complex **4** was also detected throughout the reaction. Analogous speciation was observed, albeit without complex **4** being detected, when the equivalent reaction was carried out in the absence of styrene (47% **2** after 5 minutes), demonstrating that styrene has no effect on ethene dissociation from complex **1** and that a discrete iron-ethyl-styrene analogue is not observed. This observation is consistent with reactions of $^{i\text{Pr}}$BIPFeCl$_2$ with excess Ph(CH$_2$)$_2$MgBr to form complex **3**, suggesting steric interactions impede the formation of an iron-alkyl-styrene complex, with any coordination being only transient. Low concentrations of iron(0)-tris-styrene complex **4** observed in the presence of styrene suggests that hydride transfer does take place and occurs through the reversible reaction of iron-ethyl-dinitrogen complex **2** with styrene. These low quantities of complex **4** are consistent with the requirement of additional EtMgBr to promote catalyst turnover. The reversibility of hydride transfer suggests that complex **2** is also in equilibrium with the α-aryl-iron($^{i\text{Pr}}$BIP) complex formed following hydride transfer. The fact that this α-aryl-iron($^{i\text{Pr}}$BIP) complex is not observed indicates that this equilibrium lies in favor of complex **2**, presumably due to the increased and unfavorable sterics of any purported ($^{i\text{Pr}}$BIP)iron-ethene-α-aryl complex. Interception of this intermediate with additional EtMgBr, by exchange of the α-aryl for an ethyl moiety, would result in the effective turnover observed with additional EtMgBr.

2.5 Reaction Kinetics

In order to probe whether a deactivation or inhibition process occurs over the course of the reaction, reaction progress kinetic analysis was carried out under "same excess" conditions.[63,64] Namely, a series of experiments were carried out in which the difference in concentration between EtMgBr and the styrene derivative was kept constant. This analysis was carried out for 2-methoxy-, 4-*tert*-butyl- and 3-methoxystyrene. For all three styrene derivatives there was no overlay between rate profiles across the series of experiments, indicating deactivation or inhibition during the reaction, consistent with the observed broadening of freeze-quenched Mössbauer spectra taken during catalysis (Section 2.3).

Despite this issue of catalyst decomposition, an initial rates approach was used to study the concentration dependence of each reagent in order to obtain some insight into the kinetics of this reaction. For all styrene derivatives studied, the reaction was found to be first order in iron catalyst, $^{i\text{Pr}}$BIPFeCl$_2$. Styrene derivatives bearing electron-donating substituents, 2-methoxy and 4-*tert*-butyl ($\sigma = -0.10$),[65,66] displayed saturation kinetics in both EtMgBr and styrene derivative. The positive effect of both reagents at lower concentrations is consistent with the reversible coordination of the styrene derivative to complex **2** (after ethene dissociation from complex **1**) followed by the reversible hydride transfer. In this case, turnover is limited by the interception of the disfavored α-aryl-iron($^{i\text{Pr}}$BIP) species with additional EtMgBr, as indicated by reactivity studies (see Section 2.4). At higher concentrations, the observed saturation kinetics in both reagents arises from ethene dissociation becoming turnover limiting, consistent with the observation of iron-ethyl-ethene complex **1** being the principle resting state during catalysis (see Section 2.3). By contrast, when bearing an electron-withdrawing group on the styrene derivative, 3-methoxy ($\sigma = 0.12$)[65,66], the reaction displays zero order kinetics with respect to EtMgBr and negative order kinetics with respect to the styrene derivative. This behavior is consistent with an inhibitory effect for the more strongly binding styrene derivative, as seen by the greater reactivity of 3-methoxy styrene in the competition experiment previously discussed (see Section 2.3). The observation of similar resting states during catalysis, by Mössbauer spectroscopy (see Section 2.3), indicates that inhibition does not occur by sequestering iron to an off-cycle species, but potentially by disrupting the hydride transfer equilibrium by substitution of the interacting alkene. The observation of roughly equimolar concentrations β-deuterostyrene, and non-deuterated product, at early time points in catalysis supports this inhibitory affect (see Supporting Information, Section 6).

2.6 Mechanism of Catalysis

Based on the kinetic, reactivity and spectroscopic/structural studies, a molecular-level mechanistic picture of the $^{i\text{Pr}}$BIP-iron catalyzed hydromagnesiation of styrene derivatives can be proposed (Scheme 5). The catalytic mechanism is initiated by reduction of the pre-catalyst with EtMgBr to produce iron-ethyl-ethene complex **1**, which has been isolated, characterized and shown to be the principle resting state during catalysis. Dissociation of ethene occurs to form intermediate **A**, which can reversibly bind dinitrogen to form the iron-ethyl-dinitrogen complex **2**, which was observed by freeze-quench Mössbauer spectroscopy. At higher concentrations of styrene and EtMgBr and as the reaction proceeds, the reversible binding of ethene (the byproduct of the hydride transfer reaction) becomes turnover-limiting, highlighted by the observation of complex **1** as the principle resting state during catalysis as well as large-scale reactions requiring nitrogen sparging for effective yields to be obtained.[13] Intermediate **A** can then reversibly coordinate a styrene derivative to provide key intermediate **B**, which undergoes a highly reversible, direct β-hydride transfer from the iron-bound ethyl group to the styrene derivative to give the iron-ethene-α-aryl species **C**. Binding both a styrene derivative and an alkyl moiety simultaneously to form a discrete and isolable species is unfavorable, as demonstrated by the isolation of iron-alkyl-dinitrogen complex **3**, as well as the observation of the analogous complex **2** in stoichiometric reactions of iron-ethyl-ethene complex **1** with styrene. By analogy, the additional sterics of the proposed α-aryl iron intermediate, complex **C**, would also be disfavored, resulting in the equilibria between these species (A↔B↔C) lying in favor of intermediate **A**. However, release of the product Grignard reagent from intermediate **C** is made effective by exchange with EtMgBr and returning to the more favorable iron-ethyl-ethene complex **1**, as supported by stoichiometric reaction studies demonstrating the requirement of EtMgBr for turnover. This exchange of an α-aryl for an ethyl moiety, which is turnover-limiting at low concentrations of styrene and EtMgBr, is irreversible. The irreversibility of this step was demonstrated by deuterium labelling experiments in which all deuterated products increased in concentration before plateauing, indicating that the α-aryl Grignard rea gent does not re-enter the catalytic cycle.

Over time the displacement of the $^{i\text{Pr}}$BIP ligand by the styrene derivative can take place to generate the iron(0)-tris-styrene complex **4**, which is proposed to occur from complex **C**. Formation of complex **4** is promoted when styrene derivatives bearing electron-withdrawing groups are used. Whilst removed from the principle catalytic cycle this species is similarly active for the hydromagnesiation of styrene derivatives. The observation of such a species suggests that styrene-stabilized iron(0) complexes may be accessible *in situ* in the absence of $^{i\text{Pr}}$BIP ligand. This type of species and the associated displacement of the bis(imino)pyridine ligand by an alkene could have implications for other alkene functionalization reactions using this ligand class. Further studies of this type of iron species, as well as the hydromagnesiation, in the absence $^{i\text{Pr}}$BIP and with other ligand frameworks will be the focus of future work.

3. CONCLUSIONS

The combination of detailed kinetic analysis, isotopic labelling and ^{57}Fe Mössbauer spectroscopy were used to examine the bis(imino)pyridine iron-catalyzed hydromagnesiation of styrene derivatives. These studies revealed $[^{i\text{Pr}}\text{BIPFe(Et)}(CH_2{=}CH_2)]^-$ **1** as the key resting state, which can undergo loss of ethene, and coordination of dinitrogen, to generate $[^{i\text{Pr}}\text{BIPFe(Et)}(N_2)]^-$ **2**. Upon loss of N_2 this complex can transiently coordinate the styrene derivative and mediate a rapid and highly reversible direct β-hydride transfer, the equilibrium for which lies in favor of $[^{i\text{Pr}}\text{BIPFe(Et)}(N_2)]^-$ **2**. Catalyst turnover is only achievable by exchange with an additional equivalent of EtMgBr to regenerate the catalyst resting state $[^{i\text{Pr}}\text{BIPFe(Et)}(CH_2{=}CH_2)]^-$ **1**. The unfavorable steric constraints of the proposed α-aryl-iron intermediate, over the course of the reaction, result in displacement of the bis(imino)pyridine ligand to form the iron(0) complex $[Fe(\eta^2\text{-styrene})_3(\kappa^1\text{-CH(CH}_3\text{)Ph)}]^-$ **4**, which is itself catalytically active via an alternative reaction pathway. Overall, these studies provide a critical mechanistic framework for iron-catalyzed hydromagnesiation to facilitate future methods development of this important class of reactions as well as other related alkene functionalization reactions.

Scheme 5. Proposed catalytic cycle for the BIPFe-catalyzed hydromagnesiation of styrene derivatives

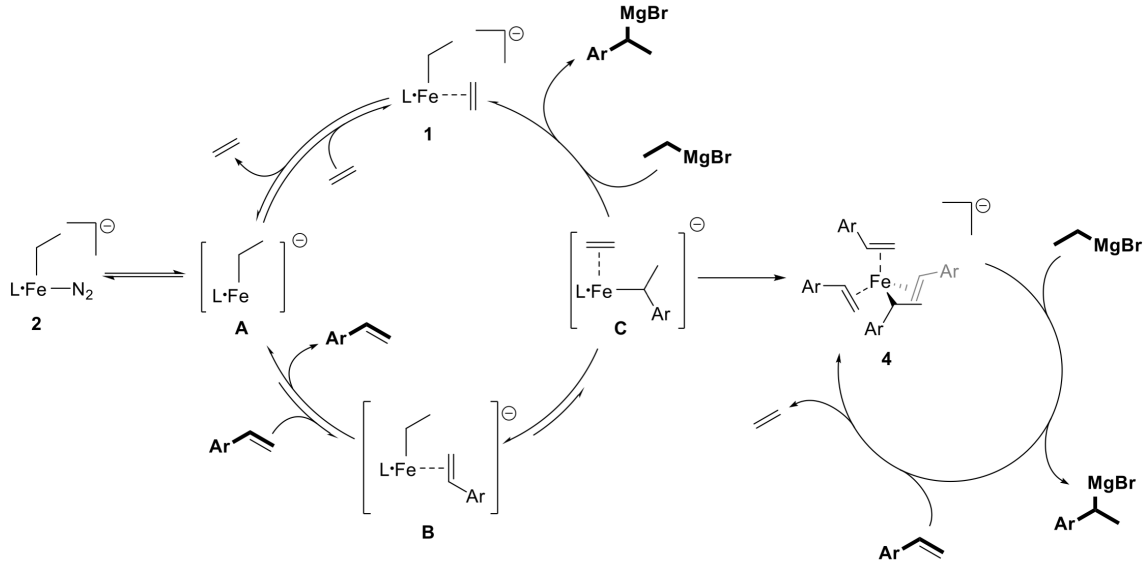

ASSOCIATED CONTENT

Supporting Information

Synthetic procedures and supplementary figures and data including ^{57}Fe Mössbauer spectra, full kinetic data and X-ray crystal structure reports is available free of charge via the Internet at http://pubs.acs.org.

AUTHOR INFORMATION

Corresponding Author

neidig@chem.rochester.edu
stephen.thomas.ed.ac.uk

Notes

The authors declare no competing financial interests.

ACKNOWLEDGMENT

This work was supported by a grant from the National Institutes of Health (R01GM111480 to M.L.N.). S.P.T. thanks the Royal Society for a University Research Fellowship. P.G.N.N thanks the Royal Society of Chemistry for a Researcher Mobility Grant. The authors would like to thank Professors Guy Lloyd-Jones and William D. Jones for helpful discussions. The NSF is gratefully acknowledged for support for the acquisition of an X-ray diffractometer (CHE-1725028).

REFERENCES

(1) Greenhalgh, M. D.; Thomas, S. P. Iron-Catalyzed Hydromagnesiation of Olefins. *Synlett* **2013**, *24* (05), 531–534.

(2) Greenhalgh, M. D.; Jones, A. S.; Thomas, S. P. Iron-Catalysed Hydrofunctionalisation of Alkenes and Alkynes. *ChemCatChem* **2014**, *7* (2), 190–222.

(3) Nakazawa, H.; Itazaki, M. Fe-H Complexes in Catalysis. *Top. Organomet. Chem.* **2011**, *33*, 27–81.

(4) Bhawal, B. N.; Morandi, B. Catalytic Transfer Functionalization through Shuttle Catalysis. *ACS Catal.* **2016**, *6* (11), 7528–7535.

(5) Silverman, G. S.; Rakita, P. E. *Handbook of Grignard Reagents*; Marcel Dekker.: New York, USA, 1996.

(6) Finkbeiner, H. L.; Cooper, G. D. Synthetic Applications of the Titanium-Catalyzed Exchange of Olefins with Grignard Reagents [1a]. *J. Org. Chem.* **1962**, *27* (10), 3395–3400.

(7) Tamura, M.; Kochi, J. Iron Catalysis in the Reaction of Grignard Reagents with Alkyl Halides. *J. Organomet. Chem.* **1971**, *31* (3), 289–309.

(8) Tamura, M.; Kochi, J. K. The Reactions of Grignard Reagents with Transition Metal Halides. *Bulletin of the Chemical Society Japan*. 1971, pp 3063–3073.

(9) Shirakawa, E.; Ikeda, D.; Masui, S.; Yoshida, M.; Hayashi, T. Iron-Copper Cooperative Catalysis in the Reactions of Alkyl Grignard Reagents: Exchange Reaction with Alkenes and Carbometalation of Alkynes. *J. Am. Chem. Soc.* **2012**, *134* (1), 272–279.

(10) Ilies, L.; Yoshida, T.; Nakamura, E. Iron-Catalyzed Chemo- and Stereoselective Hydromagnesiation of Diarylalkynes and Diynes. *J. Am. Chem. Soc.* **2012**, *134* (41), 16951–16954.

(11) Greenhalgh, M. D.; Thomas, S. P. Iron-Catalyzed, Highly Regioselective Synthesis of α-Aryl Carboxylic Acids from Styrene Derivatives and CO_2. *J. Am. Chem. Soc.* **2012**, *134* (29), 11900–11903.

(12) Jones, A. S.; Paliga, J. F.; Greenhalgh, M. D.; Quibell, J. M.; Steven, A.; Thomas, S. P. Broad Scope Hydrofunctionalization of Styrene Derivatives Using Iron-Catalyzed Hydromagnesiation. *Org. Lett.* **2014**, *16* (22), 5964–5967.

(13) Greenhalgh, M. D.; Kolodziej, A.; Sinclair, F.; Thomas, S. P. Iron-Catalyzed Hydromagnesiation: Synthesis and Characterization of Benzylic Grignard Reagent Intermediate and Application in the Synthesis of Ibuprofen. *Organometallics* **2014**, *33* (20), 5811–5819.

(14) Zhang, D.; Ready, J. M.; and, D. Z.; Ready*, J. M. Iron-Catalyzed Carbometalation of Propargylic and Homopropargylic Alcohols. *J. Am. Chem. Soc.* **2006**, *128* (47), 15050–15051.

(15) Shirakawa, E.; Yamagami, T.; Kimura, T.; Yamaguchi, S.; Hayashi, T. Arylmagnesiation of Alkynes Catalyzed Cooperatively by Iron and Copper Complexes. *J. Am. Chem. Soc.* **2005**, *127* (49), 17164–17165.

(16) Ito, S.; Itoh, T.; Nakamura, M. Diastereoselective Carbometalation of Oxa- and Azabicyclic Alkenes under Iron Catalysis. *Angew. Chemie Int. Ed.* **2011**, *50* (2), 454–457.

(17) Czaplik, W. M.; Grupe, S.; Mayer, M.; Wangelin, A. J. von. Practical Iron-Catalyzed Dehalogenation of Aryl Halides. *Chem. Commun.* **2010**, *46* (34), 6350.

(18) Bauer, I.; Knoelker, H.-J. Iron Catalysis in Organic Synthesis. *Chem. Rev. (Washington, DC, United States)* **2015**, *115* (9), 3170–3387.

(19) Sherry, B. D.; Fürstner, A. The Promise and Challenge of Iron-Catalyzed Cross Coupling. *Acc. Chem. Res.* **2008**, *41* (11), 1500–1511.

(20) Mako, T. L.; Byers, J. A. Recent Advances in Iron-Catalysed Cross Coupling Reactions and Their Mechanistic Underpinning. *Inorg. Chem. Front.* **2016**, *3* (6).

(21) Bedford, R. B.; Brenner, P. B. The Development of Iron Catalysts for Cross-Coupling Reactions. In *Iron Catalysis II*; Bauer, E., Ed.; Springer International Publishing: Cham, 2015; pp 19–46.

(22) Obligacion, J. V; Chirik, P. J. Earth-Abundant Transition Metal Catalysts for Alkene Hydrosilylation and Hydroboration. *Nat. Rev. Chem.* **2018**, *2* (5), 15–34.

(23) Shirakawa, E.; Ikeda, D.; Yamaguchi, S.; Hayashi, T. Fe-Cu Cooperative Catalysis in the Isomerization of Alkyl Grignard Reagents. *Chem. Commun. (Camb).* **2008**, No. 10, 1214–1216.

(24) Vela, J.; Smith, J. M.; Lachicotte, R. J.; Holland, P. L. Alkyl Isomerisation in Three-Coordinate Iron(Ii) Complexes. *Chem. Commun.* **2002**, No. 23, 2886–2887.

(25) Vela, J.; Vaddadi, S.; Cundari, T. R.; Smith, J. M.; Gregory, E. A.; Lachicotte, R. J.; Flaschenriem, C. J.; Holland, P. L. Reversible Beta-Hydrogen Elimination of Three-Coordinate Iron(II) Alkyl Complexes: Mechanistic and Thermodynamic Studies. *Organometallics* **2004**, *23* (22), 5226–5239.

(26) Ren, Q.; Wu, N.; Cai, Y.; Fang, J. DFT Study of the Mechanisms of Iron-Catalyzed Regioselective Synthesis of α-Aryl Carboxylic Acids from Styrene Derivatives and CO2. *Organometallics* **2016**, *35* (23), 3932–3938.

(27) Farády, L.; Bencze, L.; Markó, L. Transition-Metal Alkyls and Hydrides. *J. Organomet. Chem.* **1967**, *10* (3), 505–510.

(28) Farady, L.; Bencze, L.; Marko, L. Transition Metal Alkyls and Hydrides VIII. Nickel Chloride Catalyzed Insertion of Ethylene into Arylmagnesium Halides. *J. Organomet. Chem.* **1969**, *17* (1), 107–116.

(29) Farády, L.; Markó, L. Transition Metal Alkyls and Hydrides X. Structure of Products Formed in the Reactions between Olefins and Grignard Reagents in the Presence of Nickel Chloride. *J. Organomet. Chem.* **1971**, *28* (2), 159–165.

(30) Anton, D. R.; Crabtree, R. H. Dibenzo[a,e]Cyclooctatetraene in a Proposed Test for Heterogeneity in Catalysts Formed from Soluble Platinum-Group Metal Complexes. *Organometallics* **1983**, *2* (7), 855–859.

(31) Anton, D. R.; Crabtree, R. H. Metalation-Resistant Ligands: Some Properties of Dibenzocyclooctatetraene Complexes of Molybdenum, Rhodium and Iridium. *Organometallics* **1983**, *2* (5), 621–627.

(32) Crabtree, R. H. Resolving Heterogeneity Problems and Impurity Artifacts in Operationally Homogeneous Transition Metal Catalysts. *Chem. Rev.* **2012**, *112* (3), 1536–1554.

(33) Fieser, L. F.; Pechet, M. M. 1,2,5,6-Dibenzcycloöctatetraene [1]. *J. Am. Chem. Soc.* **1946**, *68* (12), 2577–2580.

(34) Gärtner, D.; Stein, A. L.; Grupe, S.; Arp, J.; Jacobi von Wangelin, A. Iron-Catalyzed Cross-Coupling of Alkenyl Acetates. *Angew. Chemie Int. Ed.* **2015**, *54* (36), 10545–10549.

(35) Gieshoff, T. N.; Welther, A.; Kessler, M. T.; Prechtl, M. H. G.;

Jacobi von Wangelin, A. Stereoselective Iron-Catalyzed Alkyne Hydrogenation in Ionic Liquids. *Chem. Commun.* **2014**, *50* (18), 2261–2264.

(36) Gieshoff, T. N.; Villa, M.; Welther, A.; Plois, M.; Chakraborty, U.; Wolf, R.; Jacobi von Wangelin, A. Iron-Catalyzed Olefin Hydrogenation at 1 Bar H 2 with a FeCl 3 –LiAlH 4 Catalyst. *Green Chem.* **2015**, *17* (3), 1408–1413.

(37) Collman, J. P.; Kosydar, K. M.; Bressan, M.; Lamanna, W.; Garrett, T. Polymer-Bound Substrates: A Method to Distinguish between Homogeneous and Heterogeneous Catalysis. *J. Am. Chem. Soc.* **1984**, *106* (9), 2569–2579.

(38) Rebek, J.; Gavina, F. Three-Phase Test for Reactive Intermediates. Cyclobutadiene. *J. Am. Chem. Soc.* **1974**, *96* (22), 7112–7114.

(39) Ashby, E. C.; Ainslie, R. D. Hydrometallation of 1-Octene with Grignard Reagents. Alkylmagnesiums and Alkylmagnesium Hydrides Catalyzed by Dicyclopentadienyltitanium Dichloride. *J. Organomet. Chem.* **1983**, *250* (1), 1–12.

(40) Karmel, C.; Chen, Z.; Hartwig, J. F. Iridium-Catalyzed Silylation of C–H Bonds in Unactivated Arenes: A Sterically Encumbered Phenanthroline Ligand Accelerates Catalysis. *J. Am. Chem. Soc.* **2019**, *141* (17), 7063–7072.

(41) Gao, Y.; Sato, F. On the Mechanism of Titanocenedichloride-Catalysed Hydromagnesiation of Alkynes with Alkyl Grignard Reagents. *J. Chem. Soc. Chem. Commun.* **1995**, *285* (6), 659.

(42) Finkbeiner, H.; Cooper, G. Communications- Titanium-Catalyzed Isomerization and Olefin-Exchange Reactions of Alkylmagnesium Halides: A Novel Method for Preparation of the Grignard Reagent. *J. Org. Chem.* **1961**, *26* (11), 4779–4780.

(43) Cooper, G. D.; Finkbeiner, H. L. Titanium-Catalyzed Rearrangement and Olefin-Exchange of Grignard Reagents [1]. *J. Org. Chem.* **1962**, *27* (5), 1493–1497.

(44) Ashby, E. C.; Smith, T. Hydrometallation of Alkenes and Alkynes with Magnesium Hydride. *J. Chem. Soc. Chem. Commun.* **1978**, No. 1, 30b.

(45) Sato, F.; Ishikawa, H.; Sato, M. Cp2TiCl2-Catalyzed Grignard Exchange Reactions with 1,3-Dienes or Styrenes. Preparation of Allylic and α-Arylethyl Grignard Reagents by a Convenient and Quantitative Method. *Tetrahedron Lett.* **1980**, *21* (4), 365–368.

(46) Sato, F.; Ishikawa, H.; Sato, M. Cp2TiCl2-Catalyzed Grignard Exchange Reactions with Acetylenes. A Convenient Method for Preparation of E-Alkenyl Grignard Reagents. *Tetrahedron Lett.* **1981**, *22* (1), 85–88.

(47) Sato, F.; Watanabe, H.; Tanaka, Y.; Yamaji, T.; Sato, M. Stereoselective Synthesis of Vinylsilanes from Alkynylsilanes via Hydromagnesiation. Application to a Synthesis of 7(E)-Dodecenyl Acetate and Dihydrojasmone. *Tetrahedron Lett.* **1983**, *24* (10), 1041–1044.

(48) Sato, F.; Katsuno, H. A Simple Route to 3-Furanyltrimethylsilane via Hydromagnesiation. *Tetrahedron Lett.* **1983**, *24* (17), 1809–1810.

(49) Sato, F. The Preparation of Grignard Reagents via the Hydromagnesation Reaction and Their Uses in Organic Synthesis. *J. Organomet. Chem.* **1985**, *285* (1), 53–64.

(50) The solution of (2-phenylethyl)magnesium bromide used in this reaction contained ~0.5 % styrene, produced during the Grignard reagent preparation from (2-bromoethyl)benzene.

(51) No isomerization detected in the presence of either cyclopentene, indene, α-methylstyrene or β-methylstyrene (all 10 mol%). 2-Methoxystyrene underwent hydromagnesiation using ethylmagnesium bromide in the presence of these same alkenes (all 10 mol%), indicating that they do not inhibit the hydromagnesiation reaction.

(52) Deng, L.; Margl, P.; Ziegler, T. Mechanistic Aspects of Ethylene Polymerization by Iron(II)−Bisimine Pyridine Catalysts: A Combined Density Functional Theory and Molecular Mechanics Study. *J. Am. Chem. Soc.* **1999**, *121* (27), 6479–6487.

(53) Errors of fit analyses for Mössbauer spectra of multicomponent mixtures are the following: $\delta \pm 0.02$; $\Delta E_Q \pm 3\%$ and quantitation of individual components ± 3% of the total iron content.

(54) Bart, S. C.; Chłopek, K.; Bill, E.; Bouwkamp, M. W.; Lobkovsky, E.; Neese, F.; Wieghardt, K.; Chirik, P. J. Electronic Structure of Bis(Imino)Pyridine Iron Dichloride, Monochloride, and Neutral Ligand Complexes: A Combined Structural, Spectroscopic, and Computational Study. *J. Am. Chem. Soc.* **2006**, *128* (42), 13901–13912.

(55) Tondreau, A. M.; Atienza, C. C. H.; Darmon, J. M.; Milsmann, C.; Hoyt, H. M.; Weller, K. J.; Nye, S. A.; Lewis, K. M.; Boyer, J.; Delis, J. G. P.; Lobkovsky, E.; Chirik, P. J. Synthesis, Electronic Structure, and Alkene Hydrosilylation Activity of Terpyridine and Bis(Imino)Pyridine Iron Dialkyl Complexes. *Organometallics* **2012**, *31* (13), 4886–4893.

(56) Tondreau, A. M.; Stieber, S. C. E.; Milsmann, C.; Lobkovsky, E.; Weyhermüller, T.; Semproni, S. P.; Chirik, P. J. Oxidation and Reduction of Bis(Imino)Pyridine Iron Dinitrogen Complexes: Evidence for Formation of a Chelate Trianion. *Inorg. Chem.* **2013**, *52* (2), 635–646.

(57) Bart, S. C.; Lobkovsky, E.; Chirik, P. J. Preparation and Molecular and Electronic Structures of Iron(0) Dinitrogen and Silane Complexes and Their Application to Catalytic Hydrogenation and Hydrosilation. *J. Am. Chem. Soc.* **2004**, *126* (42), 13794–13807.

(58) Stieber, S. C. E.; Milsmann, C.; Hoyt, J. M.; Turner, Z. R.; Finkelstein, K. D.; Wieghardt, K.; DeBeer, S.; Chirik, P. J. Bis(Imino)Pyridine Iron Dinitrogen Compounds Revisited: Differences in Electronic Structure Between Four- and Five-Coordinate Derivatives. *Inorg. Chem.* **2012**, *51* (6), 3770–3785.

(59) Harmony, M. D. Chapter 1 Molecular Structure Determination from Spectroscopic Data Using Scaled Moments of Inertia. In *Equilibrium Structural Parameters*; Durig, J. R. B. T.-V. S. and S., Ed.; Elsevier, 1999; Vol. 24, pp 1–83.

(60) Casitas, A.; Krause, H.; Goddard, R.; Fürstner, A. Elementary Steps of Iron Catalysis: Exploring the Links between Iron Alkyl and Iron Olefin Complexes for Their Relevance in C H Activation and C C Bond Formation. *Angew. Chemie Int. Ed.* **2015**, *54* (5), 1521–1526.

(61) Casitas, A.; Krause, H.; Lutz, S.; Goddard, R.; Bill, E.; Fürstner, A. Ligand Exchange on and Allylic C–H Activation by Iron(0) Fragments: π-Complexes, Allyliron Species, and Metallacycles. *Organometallics* **2018**, *37* (5), 729–739.

(62) Yu, Y.; Smith, J. M.; Flaschenriem, C. J.; Holland, P. L. Binding Affinity of Alkynes and Alkenes to Low-Coordinate Iron. *Inorg. Chem.* **2006**, *45* (15), 5742–5751.

(63) Blackmond, D. G. Reaction Progress Kinetic Analysis: A Powerful Methodology for Mechanistic Studies of Complex Catalytic Reactions. *Angew. Chemie Int. Ed.* **2005**, *44* (28), 4302–4320.

(64) Blackmond, D. G. Kinetic Profiling of Catalytic Organic Reactions as a Mechanistic Tool. *J. Am. Chem. Soc.* **2015**, *137* (34), 10852–10866.

(65) McDANIEL, D. H.; BROWN, H. C. An Extended Table of Hammett Substitutent Constants Based on the Ionization of Substituted Benzoic Acids. *J. Org. Chem.* **1958**, *23* (3), 420–427.

(66) Hansch, C.; Leo, A.; Taft, R. W. A Survey of Hammett Substituent Constants and Resonance and Field Parameters. *Chem. Rev.* **1991**, *91* (2), 165–195.

TOC Figure

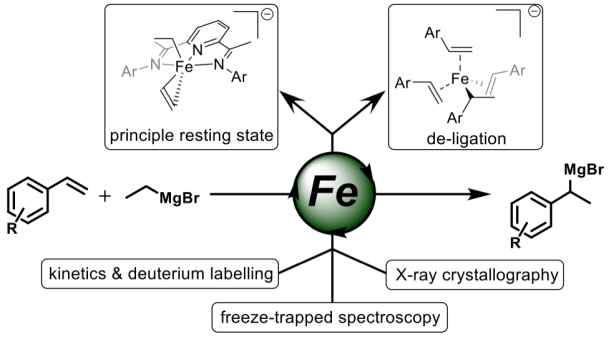
principle resting state
de-ligation
MgBr
Fe
MgBr
R
R
kinetics & deuterium labelling
X-ray crystallography
freeze-trapped spectroscopy